ap

Asian Journal of Physics
Vol. 26, No 1 (2017) 59-68
Available on: www.asianjournalofphysics.in

Study of spatial distribution of large ion clouds and the influence of geometrical perturbations in order to efficiently trap short lived radioactive nuclei in a Paul trap

Pushpa M Rao
Atomic and Molecular Physics Division
Bhabha Atomic Research Centre, Mumbai 400 085, India

Ions can be confined within the stability region over a wide range of applied potentials as here they would exhibit stable trajectories. But in the case of a large number of trapped ions, several types of interactions and perturbations play a vital role, leading to shift in the stability region and also a change in the ion oscillation frequencies. A review of the detailed study of the dynamics and behavior of large ion clouds and the effect of geometrical perturbations leading to a non-ideal trap is presented. These studies are a prerequisite to, efficient trapping and detection of relatively short lived radioactive ^{146}Eu generated at the accelerator site which is also reviewed in this paper. Studies of the mass dependent ion oscillation frequencies show that the ions trapped have a mass number 146 amu and this was confirmed by similar measurements carried out on trapped barium and potassium ions. A review of the studies of spatial density distributions of large ion cloud is also presented. These studies help in obtaining the most suitable trapping potential so that the maximum path length for Laser- ion cloud interaction is achieved thereby increasing the detection sensitivity enormously.

Keywords: Ion Trap, Ion Cloud, Ion Oscillation frequency

1 Introduction

Ion traps are an efficient tool for confinement of even a minute quantity of rare unstable radioactive isotopes, and precise atomic and nuclear measurements can be carried out as it allows long storage times [1]. For precise measurements studies have to be conducted on a single near stationary particle which is an ideal scenario requiring sophisticated set of equipments [2]. Several studies, however have been conducted on an ensemble of trapped ions world over [3,4].

The other aspect needed for precise measurements is the generation of the pure quadrupolar field, leading to the ever improvement in the design of the ion trap itself [5]. For an ideal 3-D Paul trap the field inside varies linearly with distance from the trap centre but manufacturing errors and several other modifications made in the trap for the convenience of specific experiments cause deviations in the potential. Any deviation from this 'ideal' quadrupole potential alters the characteristics of the trapped ions, manifesting as nonlinear effects. In the case of large ion clouds the main effect that needs to be considered is the shift in secular frequencies, due to nonlinearities in the trapping field [6]. In a non ideal ion trap, the ions experience a non linear field resulting in the shift in its secular ion frequency as compared to that seen in an ideal trap [7]. The changes in the trapped ion characteristics when they are subjected to a slightly asymmetric potential caused due to geometric modifications is reviewed in the present article [6].

Studies of the dynamics of large ion clouds (>10^5) has been presented in our earlier work [8]. The spatial distribution of large ion clouds (>10^6) before it attains the quasi stationary equilibrium (i.e. when

Corresponding author
e-mail: pushpam@barc.gov.in (Pushpa M Rao)

the kinetic energy of the ions is nearly a constant with time), has not been studied earlier. This is interesting because the signal to noise (S/N) ratio for large ion clouds is expected to be good but it is important to know the spatial density distribution. Besides, when large number of ions is in a non-quasi stationary equilibrium, space charge effects and rate of ion loss are prominent, detailed study of which will lead to important information about the evolution of the state of equilibrium. In our earlier studies [8] employing buffer gas cooling, the spatial ion cloud distribution for large number of ions ($>10^6$) was studied at three different potential well depths, where the ion cloud shape was expected to be near, spherical, oblate or prolate. Theoretical simulations confirmed the experimental findings [8].

The most efficient utilization and studies on minute quantities of stable/rare isotopes is possible by confining them in an ion trap. It offers long storage times of trapped ions permitting continuous probing and manipulation of atomic ions. Trapping and cooling of ions allows an innovative way to study the atomic and nuclear properties [9]. Several techniques to capture externally created ions with reasonable efficiency allow rare species such as radioactive ions [10], and highly-charged ions [11] to be extensively investigated. In recent times, nuclear physics experiments are being performed by using a combination of accelerators and ion trap facilities. The stable/unstable isotopes generated at nuclear site can be loaded either online into the traps [12] or are investigated offline by implantation of the generated isotopes onto a suitable filament and then loaded into an ion trap [13].

A technique of transferring relatively short-lived isotope of Eu^+ (4.61 days) and successfully trapping in a Paul trap facility has been reported in our earlier work [14]. In this technique, parent ^{146}Gd having longer half-life (48.27 days) was produced via an alpha induced reaction on ^{144}Sm target which produced ^{146}Eu by beta decay process. The recoil ^{146}Gd produced was first collected on an aluminum catcher which was radio-chemically separated [15] and transported to the Paul trap facility laboratory. Subsequently, $^{146}Eu^+$ was loaded in the Paul trap successfully and the trapped ions were detected using non resonant electronic technique and a review of this in conjunction with the earlier research is presented in this article.

2 Equations of motion

In the Paul trap ions are confined using a combination of DC electric field potential and the RF potential [16] and is given as

$$\phi = \frac{U_{dc} + V_{ac}\cos\Omega t}{2r_0^2}(2z^2 - x^2 - y^2) \tag{1}$$

where U_{dc} and V_{ac} are amplitudes of DC and RF potentials, respectively, Ω is RF drive frequency and x, y and z denote the position Cartesian coordinates. The distance of the end cap from center of the trap is z_o, the radius of ring electrode is $r_0 = \sqrt{2}z_0$ and m is the mass of the ion.

The time dependent force leads to the equations of motion which is in the form of Mathieu equations given as,

$$\frac{d^2u_i}{d\tau^2} + (a_i - 2q_i\cos\Omega\tau)\,u_i = 0 \tag{2}$$

where i represents the position coordinates in the x, y and z directions and a, q, $\tau = \Omega t/2$ are the dimensionless parameters.

$$a_z = \frac{8qU_{dc}}{mr_0^2\Omega^2},\ a_x = a_y = -\frac{4qU_{dc}}{mr_0^2\Omega^2} \tag{3}$$

$$q_z = \frac{4qV_{rf}}{mr_0^2\Omega^2},\ q_x = q_y = -\frac{2qV_{rf}}{mr_0^2\Omega^2} \tag{4}$$

According to the pseudopotential model [17] the stable ion oscillations comprise mainly of a slow macromotion modulated by the fast micromotion. From this model the potential well depths D_z and D_r in the z and r directions are given as follows:

$$D_z = \frac{m\Omega^2}{8q}\beta_z^2 z_0^2,\ D_r = \frac{m\Omega^2}{8q}\beta_r^2 z_0^2 \tag{5}$$

And macro-motion frequencies are given as,

$$\omega_z = \frac{1}{2}\beta_z \Omega,\ \omega_r = \frac{1}{2}\beta_r \Omega \tag{6}$$

where $\beta_{r,z}$ are continuous functions and when a and q are << 1

$$\beta_{r,z} = \sqrt{a_{(r,z)} + q^2_{(r,z)}/2} \tag{7}$$

The solutions of Eq (2) represent the motion of ion in the trap comprised of the secular motion modulated at the drive frequency (Ω). The secular motional frequency (ω_i) depends on the mass, charge of trapped species and operating parameters of the trap. In the pseudo potential well model [17], the secular frequency ω_i is expressed as function of a parameter β_i, which is a function of a_i and q_i defined in Eqs (3) and (4). For small values of a_i and q_i (< 0.4) the parameter β_i is approximated to $\sqrt{a + q^2/2}$. In other cases β_i can be written as a solution of a continuous function in a_i and q_i [16, 18]. The expression (1) describing the potential in the Paul trap is applicable only for an ideal trap and any imperfections call for modifications.

3 Experimental

The experimental set up used in all the studies reviewed here is similar to that reported in our earlier paper [19]. The ion trap used consists of a set of three hyperbolically shaped electrodes. The ring electrode radius (r_0) is 20 mm and the distance of the end-caps from the trap center is normally maintained at $r_0/\sqrt{2}$. The ring electrode has four symmetrically positioned holes each measuring 8 mm in diameter to facilitate steering of the laser beam within the ion trap. The upper end cap is in the form of a mesh to allow collection of fluorescence light from the trapped ions and the lower end cap has a slot for insertion of the filament. The lower end-cap has two rectangular slots to place filaments within the trap. The drive frequency $\Omega/2\pi$ was kept fixed at 500 KHz and the DC and RF potentials were varied to get the requisite operating parameters that define the potential well depths in the r and z directions. Stable (A = 151 and 153) Europium (Eu^+) ions were loaded in the trap by surface ionization of the sample placed on the filament. The base vacuum attained in the trap assembly was 5×10^{-9} torr. Nitrogen was used as a buffer gas for cooling the ions and the background pressure in the trap was maintained typically at 10^{-4} mbar.

The trapped ions are non-destructively detected [19] by excitation of the motional frequencies using a weak RF field applied across a high impedance tank (2MΩ) circuit at its resonance frequency. This tank circuit is connected across the end-caps of the trap. Figure 1 shows the schematic of the trapping and detection setup. The ion oscillation frequency is swept across the excitation frequency which is tuned to the resonance of the tank circuit (~55.5kHz) by varying the DC potential (U_{dc}). At resonance, damping of the excitation voltage across the tank circuit takes place and this signal is recorded. The number of ions confined in the trap is estimated from the fitting of the signal obtained to the response signal of an equivalent circuitry of trapped ions; in most of the experiments carried out presented in this paper, the number of ions confined is estimated to be ~10^6.

The other method adopted for detection of ions is Laser excited fluorescence detection. The confined ions were resonantly excited using the Nd -Yag pumped tunable dye laser system, and the resulting fluorescence was detected, and the schematic is shown in Fig 2 [20]. The laser beam has a pulse width of 25ns, pulse repetition rate of 10Hz and laser line width was 1.6 GHz. The resonance transition of Eu ions at

381.7 nm was excited from ground state $4f^7$ ($^8S_{7/2}$) $6s^9S_4$ to upper state, $4f^7$ ($^8S_{7/2}$) $6p_{3/2}$, J = 5, using the dye laser with Exalite-384 dye. The ions in the excited state partially decay to the metastable levels $4f^7(^8S_{7/2})$ $5d^9D_{4\text{-}6}$, emitting 630.3, 643.8 and 664.5 nm photons respectively. The Laser excited fluorescence photons were detected using a Ga-As Photomultiplier. The overall optical detection efficiency was ~ 0.07%. Nitrogen used as a buffer gas has a dual purpose; it cools the trapped ions via collisions and also quenches the ^9D metastable states which in turn help's in improving the S/N ratio.

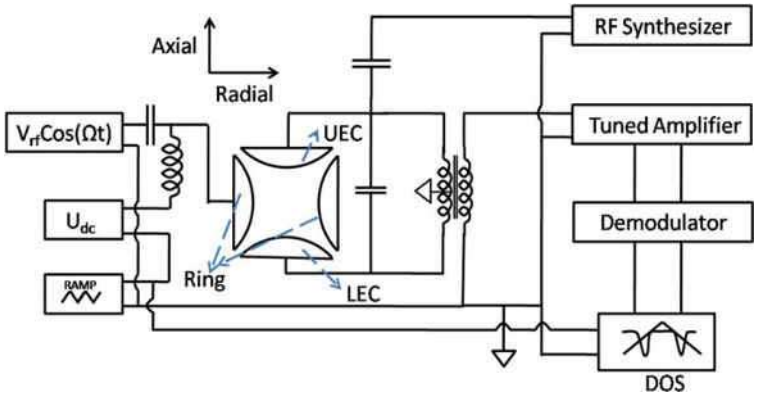

Fig 1. Electronic detection circuit schematic LEC-Lower end cap, UEC-Upper end cap

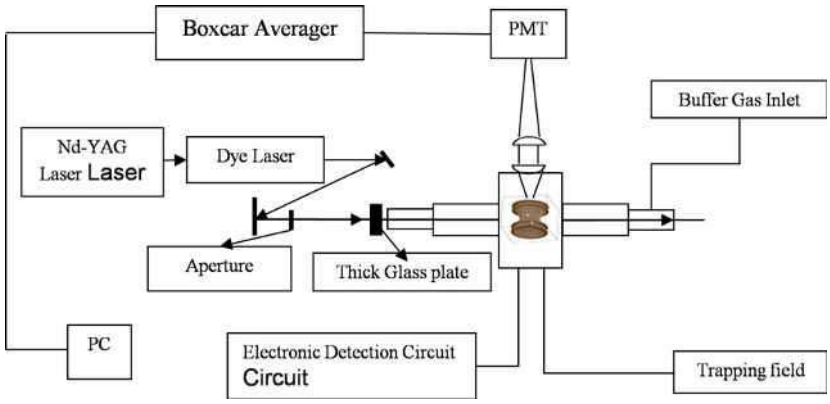

Fig 2. Schematic of the Laser excited fluorescence detection system

4 Results and Discussion

(*i*) *Influence of geometrical perturbations on trapped ion oscillation frequencies*

For precise measurements in ion traps the purity of the quadrupole potential is a prerequisite. Studies have been carried out to understand the effects of the geometrical perturbations on the dynamics of the ions trapped. The filament inserted into the lower end cap perturbs the quadrupole field and basically its effect on the ion oscillation frequency is important and this has been studied in our earlier work [6]. For a single ion in an ideal trap the motional frequencies depend solely upon the mass, operating parameters and trap dimensions but get modified due to the presence of other ions and aberrations in the trap geometry. Several researchers have shown that when ions are collectively excited, the motional resonances do not depend on the number of trapped ions i.e., no observable shift in the motional resonance frequency is seen due to the space charge effect [21, 22].

The effect of geometrical perturbations on the ion oscillation frequency is detailed in our earlier work [6] and some relevant aspects have been taken from the same for this article. The lower end-cap in the ion trap has two symmetric rectangular slots to place the filaments and the slots are positioned at 5mm distance from the center of the lower end-cap (See Fig 1b of ref [6]). A filament of dimensions 22 mm × 4 mm is inserted within the trapping region through one of the slots while the other one is kept empty. To observe the perturbation of the potential due to changes in the trap geometry, the height of the filament is changed for each set of the experiments. The DC and RF potentials were chosen in a way such that the operating parameters (a_i, q_i) are well within the stability region and the trapped ions are non-destructively detected [19]. Then a set of operating potentials (V_{rf} and U_{dc}) is followed for which the resonant excitation signal occurs at 55.6 kHz (also known as equifrequency lines within the stability region). The presence of a small quadrupolar contribution in dipolar mode of excitation enables the resonant excitation and detection of the ion oscillations, both, in axial and radial directions. The equi-frequency lines (at ~55.6 kHz) in both the axial and radial directions were obtained experimentally. This was compared with the set of potentials that were evaluated using the pseudo potential model for an ideal trap, (see Fig 3. in Ref [6]). It is clearly seen that the experimental ion oscillation frequencies differ from those calculated for an ideal trap. We have seen that the calculated ion oscillation frequency for a given set of potential at which resonant excitation signal was seen (#1 and #2 in Fig 3 of Ref [6]), differs by approximately 14 kHz from the excitation frequency. This implies that the expression used to theoretically calculate the ion oscillation frequencies has to be modified.

For a better understanding theoretical simulations were carried out using the near exact form of the potential inside the trap obtained by including the geometrical aberrations caused by insertion of the filament [6]. Using SIMION software the potential generated within the ion trap used in the experiments was simulated. The 3D potential generated is then fitted to an analytical expression which is a series expansion of the generalized potential given as

$$\phi = \phi_0 \left\{ \alpha_0 + \frac{\alpha_1 x + \beta_1 y + \gamma_1 z}{d} + \frac{\alpha_2 x^2 + \beta_2 y^2 - 2\gamma_2 z^2}{d^2} + \alpha_3 (r/d)^3 P_3(\cos(\theta)) + \alpha_4 (r/d)^4 P_4(\cos(\theta)) \right\} \tag{8}$$

where ϕ_0 is the potential applied at the ring electrode with the end-caps electrically grounded. Cartesian coordinates x, y and z are the position coordinates within the trapping volume considering the trap center as origin. In the above equation the coefficients α, β and γ represents the strength of the multipolar terms of the potential [16]. In accordance with the experimental data, the theoretical simulations have been carried out with the filament kept at the same potential as the end-caps. Trapped ion trajectories are computed by solving the equations of motion numerically using Runge Kutta 4 code with the potential given in Eq (8). Motional frequencies are then evaluated from the Fourier transformation of the simulated ion trajectories for a given set of trapping potentials and are seen to be closer to the values corresponding to the tank circuit resonance frequency (55.6 kHz).

The experiments and simulations were repeated for different insertion heights of the filament. For this study the excitation frequency was kept at 54.41 kHz and the equi-frequency lines were scanned (See Fig. 4 of Ref [6]). The Figure shows the set of operating potentials followed along each eqi-frequency line for different filament insertion heights. The continuous line represents the set of potentials evaluated for an ideal trap using pseudo potential model, for which the axial motional frequency is taken as 54.4 kHz. It can be seen that the lines move towards right (towards the black continuous theoretical curve shown in Fig 4 of Ref [6]) as the filament was placed closer to the lower end-cap. At the point where the filament was placed within the slot, the equi-frequency line moves to the other side of the theoretical line. This is quite understandable because the theoretical curve is evaluated for the case of a single ion but the experimental studies are performed on an

ion cloud showing that the space charge effects need to be considered. From earlier studies [23] it is seen that the space charge lowers the ion oscillation frequency for individual ion motion. Thus to overcome the space charge effect we expect the experimental set of potentials to move towards the right side (Fig 4 of Ref [6]), where intuitively higher ion oscillation frequency is expected. In other words the ion oscillation frequency decreases due to space charge effects and to compensate for this decrease higher U_{dc} and V_{rf} voltages need to be applied so as to detect the ions at the fixed detection frequency of 54.4 kHz (the continuous black curve). From the studies it is evident that when the filament is placed well within the slot at lower end-cap it represents the almost near ideal quadrupolar field that can be achieved experimentally. In this case the shift in equi-frequency line is solely due to the space charge effect.

To see the extent of geometrical aberration and its effect on the ion oscillation frequency the operating potential was kept a constant (V_{rf} = 550 V and U_{dc} = 21.7 V) and the axial ion oscillation frequencies were evaluated for different filament insertion heights (See Fig 10 of [6]). The figure shows the variation of the simulated ion oscillation frequencies with filament insertion heights. The oscillation frequency increases as a function of filament insertion height. This is because as the filament is moved towards the trap center, the changes in the potential are more pronounced. We see that greater the filament insertion within the trap larger is the geometrical perturbation leading to increasing shift in the individual ion oscillation frequency. Intuitively, when the filament is placed within the slot the values should have matched with the theory, however this was not the case. This discrepancy is attributed to the space charge effects. So from these studies the ideal scenario is when the filament is placed within the slot and also confine less number of ions in order to reduce the space charge effect.

(*ii*) *Study of spatial distribution of large ion clouds*

On the one hand large ion cloud is advantageous for a better S/N ratio but it calls for several corrections and approximations to achieve and report high accuracy and precision. Evolution of isotropic and anisotropic ion cloud shapes in an ion trap has been studied in our earlier work [8] and a review of some relevant portions is being described in this paper. As is clear from the earlier section apart from the geometrical perturbation space charge interaction also shifts the ion oscillation frequency. This means one has to work with less number of ions. A trade off between the S/N ratio and the space charge is inevitable. Here the main aim was to determine the trap operating parameters in order to achieve the best S/N ratio for the Laser excited fluorescence detection. Both, collisions with a light buffer gas and loss of ions result in cooling of the ions. We have tried to understand and distinguish between the two effects [8].

The experiments [8] are typically performed at three sets of operating points which decides the potential well depth in the '*r*' and '*z*' direction depending on which, the cloud shape would be spherical, prolate or oblate [24]. The dynamics of the large ion cloud was not completely understood as the ions are supposedly in a quasi continuous state where the kinetic energy of the ions are by and large a constant with time and it is important to know the evolution of the equilibrium state. The ring electrode in the ion trap has two holes of 8 mm dia diametrically opposite and the central portion of the laser beam of 1 mm in size was optimally aligned to minimize the scattered light. The Laser beam was used to scan the trapped ion cloud both along the '*x*' and '*y*' directions with fine step widths.

Essentially at three sets of operating parameters the experimental data was acquired with all other conditions kept the same, like the base vacuum, the buffer gas pressure, the filament current, the sample loading time and the laser power. Initially before scanning, the laser wavelength was fixed at the peak of the S-P transition of Eu ion and the laser excited fluorescence photons were detected by a Ga-As photomutiplier processed by a box-car average and recorded [8].

As mentioned earlier, choosing the appropriate potentials both isotropic and anisotropic cloud distributions were achieved and studied experimentally and also by theoretical simulations [8]. It is

interesting to study the ion dynamics when it is in a non-quasi state of equilibrium i.e. when the ions are loaded continuously up to saturation. By setting the operating point such that the potential well depth in the '*r*' direction is twice as that in the '*z*' direction ($D_r = 2D_z$) a spherical isotropic ion cloud distribution was achieved. Using the pseudo potential well model the calculated macromotion frequencies, are identical in both the directions, $\omega_r = \omega_z = 56.3$ kHz. From the expression of density distribution of the ion cloud put forward by various researchers [3, 24] and the fluorescence intensity expression, the radius of the ion cloud in the '*x*' and '*z*' directions Δx and Δz have been evaluated. It is seen that when the trap is operated at the potential well depth $D_x = 2D_z = 39.80$ eV the widths obtained from the Gaussian fit to the experimental data is isotopic. From this the radius of the ion cloud (See Figs 2a and 2b of [8]) in the two directions obtained is $\Delta x = \Delta z = 5.75/\sqrt{2}$ (±0.05). At the same operating point the laser scanning was performed in the '*x*' direction at different time intervals at 80 s , 260 s and 420 s after the initial loading (See Fig 3 of [8]). This points to ions undergoing evaporating cooling as the width of the ion cloud in both the directions decreases with time and there is an overall decrease in the cloud size. The time scale over which Buffer gas cooling is effective varies according to several researchers is [24-26]. Experiments were conducted in order to distinguish between the two cooling mechanisms viz., the buffer gas and evaporative cooling. Our studies show that initially the cooling of ions is due to both the mechanisms and with time it is seen that evaporative cooling is the more effective.

By choosing operating parameters such that $D_x < 2D_z$ an anisotropic spatial distribution of the ion cloud in an oblate form has been be realized, and in this case the ion oscillation frequency in the two directions are such that $\omega_r < \omega_z$. Along the same lines when $D_x > 2D_z$ a prolate ion cloud is realized and in this case $\omega_r > \omega_z$. In both cases the widths of the ion cloud has been evaluated from the data obtained by scanning the ion cloud in the '*x*' and '*z*' directions and it is seen from the aspect ratio $\Delta z / \Delta x$ that the ion cloud tends to attain a more oblate or prolate shape with time as a result of cooling of ions. Theoretical simulations using a Monte Carlo code was performed on 1000 ions where the parabolic pseudo potential was taken as the trapping potential and the coulomb repulsion term experienced by each ion due to the rest of the ions was included for space charge effects [8]. The spatial density distribution of the simulated ion cloud compares well with the experimental measurements (See Fig 6a,b,c of Ref [8]).

From these studies we also infer that when the trap is operated at the potentials such that we generate an oblate ion cloud the fluorescence signal strength is the maximum which is obvious as the laser interaction path length with the ion cloud is maximum in this case.

(*iii*) *Trapping of relatively short-lived radioactive* ^{146}*Eu in a Paul trap*

A new technique has been developed for transferring one of the relatively short lived isotopes of europium (^{146}Eu, Half life = 4.61 days) into the Paul ion trap.

The relatively short-lived isotope of Eu^+ (4.61 days) was transferred and successfully trapped in a Paul trap facility [14]. In this technique, parent ^{146}Gd having longer half-life (48.27 days) was produced via an alpha induced reaction on ^{144}Sm target which produced ^{146}Eu by beta decay process. The recoil ^{146}Gd nuclei was initially collected on an Aluminum catcher and was later radiochemically separated [15]. This was finally loaded into the Paul ion trap facility.

As described earlier the lower end cap has two slots for placing the filaments. On one of the Pt filament which was shaped in the form of a boat, the concentrated solution of ^{146}Gd/^{146}Eu atoms was dropped through a micropipette and dried under an Infra-Red lamp. The filament contained approximately 6×10^{10} number of ^{146}Gd atoms. On the other filament a sample of Barium chloride was placed in order to perform comparative studies. The chamber containing the Paul trap set up was evacuated to ultra high vacuum (1×10^{-9} mbar). The short lived ^{146}Eu undergoes beta decay via ($^{146}Eu \rightarrow {}^{146}Sm + \beta^+$) and produces ^{146}Sm,

and the trapping experiment was started after 17 days of irradiation when the ^{146}Eu yield was expected to be maximum. Subsequently, $^{146}Eu^{+}$ was loaded in the Paul trap by surface ionization and the trapped ions were detected using non destructive resonant electronic technique [14].

In this experiment the geometrical perturbations which has an effect on the ion oscillation frequency was minimized as inferred from the studies described in the first section. The confined short lived ^{146}Eu isotope was detected by a non destructive method. Here, the response of the mass dependent trapped ion oscillation frequency is measured via the weak probing dipole field applied across the tank circuit (Q value ~100) which is coupled to the ion trap as described earlier in Section 3.

The effect of charge to mass ratio on the ion oscillation frequency manifests into the fact that the equi- frequency lines are different for different ion species. This was experimentally confirmed by following the equi-frequency lines at different set of trapping potentials (V_{ac} and U_{dc} trapping) for three different ion mass numbers (See Fig 3 of Ref [14]). When $^{138}Ba^{+}$ is trapped at a given set of trapping potentials, it follows an equi-frequency line different from $^{146}Eu^{+}$. We also observed similar result for $^{39}K^{+}$ which was an impurity element present in the Ba sample. For ^{138}Ba and ^{39}K ions the equi-frequency line was followed for several sets of operating points V_{ac} and U_{dc}. While for ^{146}Eu ions, due to small quantity of sample, it was loaded at an optimum operating point and the experiment was performed several times at the same set of applied potential. Keeping the axial ion oscillation frequency fixed at 54.5 kHz, the trapping potentials were theoretically evaluated for the three different ion species i.e. ^{146}Eu, ^{138}Ba and ^{39}K and this is seen to match well with the experimental results (See Fig 3 of Ref [14]). This confirms that we have trapped and detected the radioactive ions with 146 atomic mass units.

The radioactive sample contains ^{146}Gd and ^{146}Sm isobaric impurities along with the ^{146}Eu isotope. The total number of trapped ions of mass 146 amu estimated from the experimental signal as described in [14] is $1.2\times10^{5}(\pm10^{4})$. Using the Langmuir-Saha equation the thermal ionization probabilities was calculated for Gd, Sm, and Eu. Gd has a higher ionization potential thus its yield compared to Eu and Sm at say 1200K is significantly lower. Combining the evaluated ionization probabilities of all the isobars, and their abundance calculated on the day the experiment the fraction of each isobaric species of mass 146 amu that is trapped was estimated. From these estimated fractions and the total number of trapped ions, the absolute number of trapped ^{146}Eu ions is estimated to be 2.4×10^{4} ($\pm\ 5\times10^{3}$).

The other method to ascertain the trapping of ^{146}Eu ions is Laser-excited fluorescence detection. In our earlier work, we described the laser-excited fluorescence detection of nearly $\sim10^{6}$ trapped Eu (stable) ions using an Nd-YAG pumped tunable dye laser system [20]. As the number of ^{146}Eu is much lesser for this part of the experiment, we carefully set the operating parameters of the trap such that applied potential yielded the potential well depths $D_x < 2D_z$. As described in the Section (*ii*)**,** formation of an oblate ion cloud was realized and it was experimentally verified that the S/N ratio is maximum when the ion cloud has an oblate shape. Now using the same experimental set up as detailed in Section (*ii*)**,**, laser-excited fluorescence of the confined ^{146}Eu ions was attempted but did not yield positive results.

In our earlier paper [14], the unsuccessful attempts to detect the laser excited fluorescence photons using an Nd-YAG pumped dye laser system has been analysed. Simulation studies were carried out on the number of photons emitted during each laser excitation pulse of the three level (S, P and D states) system of the Eu ion. From the simulations it is inferred that it is difficult to detect 2.4×10^{4} trapped europium ions optically using a pulsed laser system and with the optical detection efficiency of 0.001 as is used in the experiment [14]. A CW laser system would definitely be the solution along with improved detection efficiency.

5 Conclusion

Geometrical aberrations occurring due to the insertion of the filament within the ion trap causes perturbations in the trapping potential and its effects on the ion oscillation frequencies has been studied. It is seen that the simulations with the perturbation terms included matches with the experimental findings as compared to an ideal trap scenario. It is noted that greater the filament insertion within the trap larger is the geometrical perturbation leading to increasing shift in the individual ion oscillation frequency. When the filament is placed well within the slot the ion oscillation frequency is shifted to the other direction and this is attributed to the space charge effects. The shift in ion oscillation frequency depends on the total number of ions trapped and also the number density (space charge effect is more pronounced here) which has been experimentally confirmed by loading more number of ions and by buffer gas cooling.

The spatial distribution of the ion cloud has been experimentally measured by changing the ratio of D_x / $2D_z$ from equal to one, greater than one and lesser than one, and it is seen that the ion cloud shape changes from spherical to prolate or oblate, respectively. The data obtained from the Laser scan of the ion cloud distribution experimentally was a good Gaussian fit from which the width of the ion cloud was evaluated. In the case of an isotropic ion cloud the widths in the '*x*' and '*z*' directions remained equal and it decreased as the ions cooled. Whereas for an anisotropic ion cloud the aspect ratio obtained by the experimental measurements got closer to the theoretically simulated values as the loss of ions and cooling set in. The S/N noise ratio of the laser excited fluorescence was seen to be maximum in the case of an oblate ion cloud distribution.

With the perturbations inside the ion trap minimized and the potential chosen such that the Laser excited fluorescence yields the best S/N ratio an efficient utilization of minute quantity of short lived ^{166}Eu isotopes was possible using the ion trapping technique. The short-lived, radioactive ^{146}Eu isotope in a Paul trap along with isobars, i.e^{146}Gd and ^{146}Sm was collected at an accelerator site and confined in a Paul trap. The equi-frequency line plot measurements confirm that species having mass 146 amu was trapped. From the calculation of number of ions generated using the surface ionization technique it is shown that most of the trapped species are ^{146}Eu and ^{146}Sm ions as their ionization potential is lower than that of Gd. The experiments confirmed that $^{146}Eu^{+}$ ions were trapped and the number was estimated to be ~2.4×10^4.

Acknowledgement

The Author wishes to thank Manoj Kumar Joshi whose underlying contribution in the all work carried out forms the basis of this article. The Author is grateful to Dr P Das for help in the effort towards production and collection of the short lived Eu isotope. The Author also wishes to thank A K Sikdar, Dr T Bhattacharjee, Dr S K Das and Dr K T Satyajit for their individual contributions.

References

1. Werth G, Hyperfine *Interact*, 172(2006)125; doi:10.1007/s10751-007-9531-6
2. Wineland D J, Bergquist J C, Itano W M, Drullinger R E, *Opt Lett*, 5 (1980) 245; doi.org/10.1364/OL.5.000245
3. Knight R D, Prior M H, *J Appl Phys*, 50(1979)3044-3049
4. Schaaf H, Schmeling U, Werth G, *Appl Phys*, 25(1981)249-251
5. Brown L S, Gabrielse G, *Rev Mod Phys*, 58(1986)233; doi: 10.1103/RevModPhys.58.233
6. Joshi Manoj Kumar, Satyajit K T, Rao Pushpa M, *Nucl Instrum Methods Phys Res A*, 800(2015)111-118
7. Franzen J, *Int J Mass Spectrom Ion Process*, 106(1991)63-78
8. Joshi Manoj Kumar, Rao Pushpa M, *Int J Mass Spectrom*, 328-329(2012)36-42
9. Bollen G, Traps for Rare Isotopes, *Lect Notes Phys*, 651(2004)169-210.
10. Stolzenberg H, Becker St, Bollen G. Kern F, Kluge H.-J, Otto T, Savard G, Schweikhard L, Audi G, Moore R B, *Phys Rev Lett*, 65(1990)3104; doi: 10.1103/PhysRevLett.65.3104

11. Bergstrom I, Borgenstrand H, Carlberg C, Rouleau G, Smith B, Schuch R, Bollen G, Jertz R, Kluge H.-J, Schark E and Schwarz T, *Phys Scrip*, 47(1993)475; doi:10.1088/0031-8949/47/3/018
12. (a) Bollen G, Traps for Rare Isotopes, *Lect Notes Phys*. 651(2004)169-210.
    (b) Mukherjee M, Beck D, Blaum K, Bollen G, Dilling J, George S, Herfurth F, Herlert A, Kellerbauer A, Kluge H.-J, Schwarz S, Schweikhard L, Yazidjian C, *Eur Phys J: A*, 35(2008)1-29.
13. Enders K, Stachowska E, Marx G, Ch Zölch, Georg U, Dembczynski J, Werth G, (ISOLDE Collaboration), *Phys Rev A*, 56(1997)265; doi.org/10.1103/PhysRevA.56.265
14. JoshiM K, Sikdar A K, Rao Pushpa M, Bhattacharjee T, Das S K, Das P, *Phys Scr*, 89(2014)085404 (7pp); doi.org/10.1088/0031-8949/89/8/085404
15. Nayak D, Lahiri S, Ramaswami A, Manohar S B, Das NR. *Appl Radiat Isot*, 51(1999)631-636.
16. Major F. G, Gheorghe, Viorica N. Werth Günther Charged Particle Traps Physics and Techniques of Charged Particle Field Confinement, Springer Seires, (2005).
17. Dehmelt H G, *Adv At Mol Phys*, 3(1967)53; doi.org/10.1016/S0065-2199(08)60170-0
18. March R E, Todd JFJ, Quadrupole Ion Trap Mass spectrometry, 2nd edn, (Willey-Interscience), 2005,165.
19. Bhattacharya S, Gupta Anita, Nakhate S G, Rao Pushpa M, *Pramana: J Phys*, 67(2006)1087; doi: 10.1007/s12043-006-0025-x
20. Rao P M, Gupta Anita, *Pramana: J Phys*, 78(2012)109-120.
21. Alheit R, Enders K, Werth G, *Appl Phys B*, 62(1996)511-513.
22. Paasche P, Valenzuela T, Biswas D, Angelescu C, Werth G, *Eur Phys J:D*, 18(2002)295-300.
23. Alheit R, Chu X Z, Hoefer M, Holzki M, Werth G, Blümel R, *Phys Rev A*, 56(1997)4023; doi.org/10.1103/PhysRevA.56.4023
24. Schaaf H, Schmeling U, Werth G, *Appl Phys*, 25(1981)249; doi:10.1007/BF00902978
25. Vedel F, Andre J, Vedel M, Brincourt G, *Phys Rev A*, 27(1983)2321; doi.org/10.1103/PhysRevA.27.2321
26. Hou J, Wang Y, Yang D, *J Appl Phys*, 88(2000)4334; doi:10.1063/1.1286232

[*Received*: 30.1.2017]